Contribution from the Departments of Chemistry, The Johns Hopkins University, Baltimore, Maryland 21218, and Emory University, Atlanta, Georgia 30322

Preparation and Structure of *cis*-[(Ethylenediamine)bis(1,3,9-trimethylxanthine)platinum(II)] Nitrate Dihydrate and *cis*-[(Ethylenediamine)bis(1,3,9-trimethylxanthine)platinum(II)] Hexafluorophosphate. Effect of Intramolecular and Intermolecular Interactions on Molecular Conformation in the Solid State

JOHN D. ORBELL,[1a] KENNETH WILKOWSKI,[1a] BALTAZAR DE CASTRO,[1a] LUIGI G. MARZILLI,*[1b] and THOMAS J. KISTENMACHER*[1a]

Received June 15, 1981

The synthesis, solution ^1H NMR spectrum, and solid-state molecular and crystal structure of *cis*-[(en)Pt(1,3,9-TMX)$_2$](NO$_3$)$_2$·2H$_2$O and *cis*-[(en)Pt(1,3,9-TMX)$_2$](PF$_6$)$_2$ (where 1,3,9-TMX = 1,3,9-trimethylxanthine) are reported. The NO_3^- salt crystallizes in the monoclinic system, space group $P2_1/c$, with a = 22.215 (24) Å, b = 7.945 (6) Å, c = 16.463 (6) Å, β = 111.91 (4)°, V = 2695.8 Å^3, Z = 4 (based on a molecular weight of 803.62 for [Pt(C$_2$H$_8$N$_2$)(C$_8$H$_{10}$N$_4$O$_2$)$_2$](NO$_3$)$_2$·2H$_2$O), D_{measd} = 1.98 (1) g cm^{-3}, and D_{calcd} = 1.98 g cm^{-3}. The PF_6^- salt also crystallizes in the monoclinic system, space group $C2/c$, with a = 14.880 (3) Å, b = 9.236 (2) Å, c = 21.810 (4) Å, β = 91.17 (1)°, V = 2996.8 Å^3, Z = 4 (based on a molecular weight of 933.50 for [Pt(C$_2$H$_8$N$_2$)(C$_8$H$_{10}$N$_4$O$_2$)$_2$](PF$_6$)$_2$), D_{measd} = 2.07 (1) g cm^{-3}, and D_{calcd} = 2.07 g cm^{-3}. Intensity data for 7320 (NO_3^- salt) and 4289 (PF_6^- salt) symmetry-independent reflections were collected by utilizing the θ-2θ scan mode on an automated diffractometer employing graphite-monochromatized Mo Kα radiation. Both structures were solved by standard heavy-atom Patterson and Fourier techniques and have been refined by full-matrix least-squares analysis (R = 0.048 and 0.044 for the NO_3^- and PF_6^- salts, respectively). The primary coordination sphere about the Pt(II) center is approximately square planar in each complex cation, with the N atoms of the en chelate and the N(7) atoms of the cis-bound 1,3,9-TMX ligands occupying the four coordination sites. Whereas in the NO_3^- salt the complex cation has only approximate 2(C_2) symmetry, such symmetry is crystallographically required for the cation in the PF_6^- salt. Principal intracomplex geometrical parameters for the NO_3^- salt are as follows: Pt-N(en) = 2.012 (4), 2.026 (3) Å; Pt-N(7) = 2.010 (3), 2.021 (4) Å; N(7)-Pt-N(7) = 89.1 (1)°; interbase dihedral angle = 70.6°; base/PtN$_4$ coordination plane dihedral angles = 116.8, 119.5°. These same parameters for the PF_6^- salt are as follows: Pt-N(en) = 2.029 (5) Å; Pt-N(7) = 2.018 (4) Å; N(7)-Pt-N(7) = 91.6 (2)°; interbase dihedral angle = 87.3°; base/PtN$_4$ dihedral angle = 121.4°. A detailed comparison is made among the conformational aspects of the present complexes and those displayed by a variety of other *cis*-bis(N(7)-bound 6-oxopurine)platinum(II) systems.

Introduction

A leading speculation as to the mode of action of cis platinum(II) antitumor drugs invokes the disruption of DNA replication by the formation of an intrastrand cross-linkage between adjacent nucleobases in regions of high guanosine-cytidine (G-C) content.[2-6] The principal binding sites for Pt(II) to guanosine and cytidine are the endocyclic nitrogen atoms N(7) and N(1) (after deprotonation) of G and the endocyclic nitrogen atom N(3) of C.[2,5,7-9] Thus, in regions of high G-C content, one may envision three main types of cross-linking modes involving the N(7) and N(1) atoms of the imidazole and pyrimidine rings, respectively, of G and the N(3) atom of C.[10] These modes may be represented as follows: (1) G[N(7)]-Pt-G[N(7)]; (2) G[N(7)]-Pt-G[N(1)] or G[N(7)]-Pt-C[N(3)]; (3) C[N(3)]-Pt-C[N(3)], C[N(3)]-Pt-G[N(1)], or G[N(1)]-Pt-G[N(1)].

In attempts to gain insight into these types of intrastrand cross-linking modes on a molecular level, many model systems have been investigated by X-ray crystallographic methods.[2,7] Such model systems usually involve the cis coordination of two nucleobase derivatives to the A$_2$Pt^{II} cationic moiety, where A = NH_3 or A$_2$ = ethylenediamine (en) or trimethylenediamine (tn). A number of models for the type 1 cross-linking mode have been structurally characterized.[2] In addition, the structure of a type 2 model cation, *cis*-[(NH$_3$)$_2$Pt(1-methylcytosine)(9-ethylguanine)]$^{2+}$, has recently been reported.[11] Structurally characterized models for the type 3 mode include the *cis*-[(NH$_3$)$_2$Pt(cytosine 3'-monophosphate)$_2$]$^{2-}$ anion[12] and a *cis*-bis(N(3)-bound ligand)Pt(II) complex with 1-methylcytosine.[7] These models exhibit a number of structurally interesting features, and we[7] have previously proposed a convention for comparing the principal conformational aspects of intrastrand cross-linking models. One feature of the type 1 models is the frequent occurrence of a significant intracomplex base/base interaction somewhat akin to the base/base stacking commonly found in polynucleobase compounds.[2] This interaction may persist in solution as evidenced by enhanced circular dichroism spectra for some *cis*-bis(6-oxopurine nucleotide) complexes.[2,3]

Since methylation of purine rings enhances base stacking in solution, we felt it would be interesting to examine type 1 models containing highly methylated bases. Furthermore, we wished to assess the influence of different counterions on the molecular conformation of cationic models. Thus, we have

(1) (a) The Johns Hopkins University. (b) Emory University.
(2) de Castro, B.; Kistenmacher, T. J.; Marzilli, L. G. In "Trace Elements in the Pathogenesis and Treatment of Inflammatory Conditions"; Rainsford, K. D., Brune, K., Whitehouse, M. W., Eds.; Agents and Actions: Basel, 1981; and references therein.
(3) (a) Marzilli, L. G.; Kistenmacher, T. J.; Eichhorn, G. L. In "Nucleic Acid-Metal Ion Interactions"; Spiro, T. G., Ed.; Wiley: New York, 1980; Chapter 5. (b) Barton, J. K.; Lippard, S. J. *Ibid.*, Chapter 2. (c) Marzilli, L. G. *Adv. Inorg. Biochem.*, in press.
(4) Cohen, G. L.; Ledner, J. A.; Bauer, W. R.; Ushay, H. M.; Caravana, C.; Lippard, S. J. *J. Am. Chem. Soc.* **1980**, *102*, 2487.
(5) Marzilli, L. G. *Prog. Inorg. Chem.* **1977**, *23*, 255.
(6) Kelman, A. D.; Buchbinder, M. *Biochimie* **1978**, *60*, 893.
(7) Orbell, J. D.; Marzilli, L. G.; Kistenmacher, T. J. *J. Am. Chem. Soc.* **1981**, *103*, 5126.
(8) Lippert, B.; Lock, C. J. L.; Speranzini, R. A. *Inorg. Chem.* **1981**, *20*, 335.
(9) Lippert, B.; Lock, C. J. L.; Speranzini, R. A. *Inorg. Chem.* **1981**, *20*, 808.
(10) Kistenmacher, T. J.; de Castro, B.; Wilkowski, K.; Marzilli, L. G. *J. Inorg. Biochem.*, in press, and references therein.
(11) Faggiani, R.; Lock, C. J. L.; Lippert, B. *J. Am. Chem. Soc.* **1980**, *102*, 5419.
(12) Wu, S. M.; Bau, R. *Biochem. Biophys. Res. Commun.* **1979**, *88*, 1435.

0020-1669/82/1321-0813$01.25/0

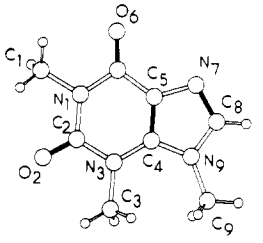

Figure 1. Molecular structure and numbering scheme for the free base 1,3,9-trimethylxanthine (1,3,9-TMX). Shaded bonds indicate bond orders greater than 1 in the resonance form presented.

Table I. Crystal Data for $[(en)Pt(1,3,9\text{-}TMX)_2](NO_3)_2 \cdot 2H_2O$ and $[(en)Pt(1,3,9\text{-}TMX)_2](PF_6)_2$

	NO_3^- salt	PF_6^- salt
a, Å	22.215 (24)	14.880 (3)
b, Å	7.945 (6)	9.236 (2)
c, Å	16.463 (6)	21.810 (4)
β, deg	111.91 (4)	91.17 (1)
V, Å^3	2695.8	2996.8
space group	$P2_1/c$	$C2/c$
mol wt	803.62	933.50
D_{measd}, g/cm^3	1.98 (1)	2.07 (1)
D_{calcd}, g/cm^3	1.98	2.07
Z	4	4

prepared and structurally characterized the nitrate and hexafluorophosphate salts of the *cis*-$[(en)Pt(1,3,9\text{-}TMX)_2]^{2+}$ cation, where 1,3,9-TMX is the modified purine base 1,3,9-trimethylxanthine (isocaffeine); see Figure 1. We have used our previously devised convention[7] to compare the primary conformational features of these two complex cations to each other and to related systems. In addition, we have characterized these isocaffeine complexes by ^1H NMR spectroscopy.

Experimental Section

Reagents. 1,3,9-TMX was purchased from Tridom/Fluka. Common chemicals were obtained from other scientific supply houses.

A. $[(en)Pt(1,3,9\text{-}TMX)_2](NO_3)_2 \cdot 2H_2O$. (a) Synthesis. An aqueous solution of $AgNO_3$ (339 mg; 2 mmol) was added to a suspension of $(en)PtI_2$[13] (509 mg; 1 mmol) in 10 mL of distilled water (total volume ~20 mL). The mixture was heated at ~60 °C (with stirring) for 2 h, and the insoluble AgI was filtered over Celite. A warm aqueous solution of 1,3,9-TMX (388 mg; 2 mmol) was added to the filtrate with stirring. After several days of slow evaporation, well-formed crystals were harvested. A density measurement (neutral buoyancy method; $CCl_4/CHBr_3$) and preliminary X-ray data were consistent with the formulation $[(en)Pt(1,3,9\text{-}TMX)_2](NO_3)_2 \cdot 2H_2O$.

(b) Collection and Reduction of the X-ray Intensity Data. Preliminary oscillation and Weissenberg photographs showed the crystal system to be monoclinic with systematic absences ($h0l$, $l = 2n + 1$; $0k0$, $k = 2n + 1$) consistent with the space group $P2_1/c$. Precise unit-cell dimensions and their associated standard deviations were derived from a least-squares fit to the setting angles for 15 carefully selected reflections on a Syntex $P\bar{1}$ automated diffractometer. The crystallographic c axis was approximately aligned along the ϕ axis of the spectrometer. Relevant crystallographic data are collected in Table I.

The intensities of 10 158 reflections were measured on the diffractometer employing graphite-monochromatized Mo Kα radiation and the θ–2θ scan mode with a constant scan speed of 1.5° min^{-1} (in 2θ). The dimensions and face assignments for the crystal used in data collection and other pertinent data collection parameters are given in Table II.

The intensities of three standards were monitored after every 97 reflections and showed no systematic variation over the course of the experiment. However, a troublesome feature was the tendency for the maxima of the standards to drift slightly about the center of the scan window. Checks on the optical alignment and recentering of the crystal four times during the experiment failed to resolve this problem. After each centering procedure, the cell dimensions were redetermined, and as there were significant variations (particularly in the magnitude of a), the final set of cell parameters quoted in Table I were obtained by averaging over the four independent sets. These problems are probably attributable to a loss of water from the crystal during data collection since only one of the two expected water molecules of crystallization per asymmetric volume could be located in the subsequent analysis.

Table II. Intensity Collection Data for $[(en)Pt(1,3,9\text{-}TMX)_2](NO_3)_2 \cdot 2H_2O$ and $[(en)Pt(1,3,9\text{-}TMX)_2](PF_6)_2$

	NO_3^- salt	PF_6^- salt
cryst dimens, mm	(001)–$(00\bar{1}) = 0.24$ (010)–$(0\bar{1}0) = 0.18$ (100)–$(\bar{1}00) = 0.18$	$(1\bar{1}0)$–$(\bar{1}10) = 0.36$ $(00\bar{1})$–$(001) = 0.35$ $(\bar{1}\bar{1}0)$–$(110) = 0.24$
2θ limits, deg	3–60	3–60
scan rate (2θ), deg/min	1.5	1.5
total data	10 158	8738
R_{av}	2.3	4.0
unique data	7909/7320 ($I > 0$)	4379/4289 ($I > 0$)
μ[λ(Mo K$\bar{\alpha}$) = 0.710 69 Å], cm^{-1}	53.9	51.4
transmission factor range	0.36–0.47	0.17–0.32

The measured intensities were symmetry averaged and reduced to a set of 7909 independent values; of these, 7320 had net intensities above zero and were assigned observational variances on the basis of the equation $[\sigma(I)]^2 = S + (B_1 + B_2)(T_S/2T_B)^2 + (pI)^2$, where S, B_1, and B_2 are the scan and extremum background counts, T_S and T_B are the scan and individual background counting times ($T_B = T_S/4$ for all reflections), and p was taken to be 0.03 and represents an estimate of the error proportional to the diffracted beam intensity.[14] Reflections with net negative intensities were assigned I's and weights equal to zero. The positive net intensities and their estimated standard deviations were corrected for Lorentz and polarization effects. An absorption correction was also applied on the basis of the crystal dimensions and face assignments given in Table II. An approximation to the absolute scale factor was derived by the method of Wilson.[15]

(c) Solution and Refinement of the Structure. The positional coordinates of the Pt atom were deduced from a three-dimensional Patterson synthesis. A subsequent structure factor Fourier calculation gave the location of 41 other nonhydrogen atoms. Only one of the two expected water molecules of crystallization could be found. Several cycles of isotropic and anisotropic least-squares refinement, minimizing the quantity $\sum w(|F_o| - |F_c|)^2$ where $w = 4F_o^2/[\sigma(F_o^2)]^2$, gave an R value ($\sum||F_o| - |F_c||/\sum|F_o|$) of 0.053. At the juncture, a difference-Fourier synthesis again failed to reveal evidence for the missing water molecule of crystallization but did yield coordinates for the 30 hydrogen atoms of the monohydrate. The isotropic temperature factor of each hydrogen atom was fixed at a value approximately 1.0 Å^2 higher than the atom to which it is bonded. The contributions from the hydrogen atoms were included in subsequent cycles of refinement, but no attempt was made to refine either positional or thermal parameters. Two further cycles of refinement led to convergence (all shift/error less than 0.7) and to a final R value of 0.048. The final weighted R $[(\sum w(|F_o| - |F_c|)^2/\sum w|F_o|^2)^{1/2}]$ and goodness-of-fit $[(\sum w(|F_o| - |F_c|)^2/(NO - NV))^{1/2}$, where NO = 7320 nonzero observations and NV = 253 variables] were 0.038 and 1.44, respectively. A final difference-Fourier synthesis revealed no peaks greater than 0.74 e/Å^3.

Neutral-atom scattering factors for the nonhydrogen atoms[16] and the hydrogen atoms[17] were taken from common sources. Anomalous dispersion corrections were applied to the scattering curves for all nonhydrogen atoms.[18] Final atomic positional parameters for the nonhydrogen atoms are collected in Table III. Tables of anisotropic thermal parameters, the hydrogen atom parameters, and final observed and calculated structure factor amplitudes are available.[19]

(13) Dhara, S. C. *Indian J. Chem.* **1970**, *8*, 193.

(14) Busing, W. R.; Levy, H. A. *J. Chem. Phys.* **1957**, *26*, 563.
(15) Wilson, A. J. C. *Nature (London)* **1942**, *150*, 152.
(16) Hanson, H. P.; Herman, F.; Lea, J. D.; Skillman, S. *Acta Crystallogr.* **1964**, *17*, 1040.
(17) Stewart, R. F.; Davidson, E. R.; Simpson, W. T. *J. Chem. Phys.* **1965**, *42*, 3175.
(18) Cromer, D. T.; Liberman, D. *J. Chem. Phys.* **1970**, *53*, 1891.
(19) See paragraph at end of the paper regarding supplementary material.

Table III. Final Nonhydrogen Atom Coordinates for $[(en)Pt(1,3,9\text{-}TMX)_2](NO_3)_2 \cdot 2H_2O$[a]

atom	x	y	z
Pt[b]	23301 (0.7)	7320 (2)	32950 (1)
N(10)	1681 (2)	591 (5)	2058 (2)
N(11)	2805 (2)	−1053 (5)	2888 (2)
C(10)	1952 (3)	−433 (7)	1512 (3)
C(11)	2349 (3)	−1828 (7)	2066 (3)
O(2A)	−449 (2)	3866 (4)	3856 (2)
O(6A)	765 (2)	−1 (4)	3086 (2)
N(1A)	169 (2)	1954 (5)	3477 (2)
N(3A)	537 (2)	4750 (5)	3881 (2)
N(7A)	1836 (2)	2613 (4)	3579 (2)
N(9A)	1656 (2)	5194 (4)	3963 (2)
C(1A)	−339 (2)	694 (7)	3390 (4)
C(2A)	55 (2)	3539 (6)	3757 (3)
C(3A)	394 (3)	6461 (6)	4086 (3)
C(4A)	1102 (2)	4277 (5)	3813 (3)
C(5A)	1209 (2)	2697 (5)	3570 (3)
C(6A)	727 (2)	1411 (5)	3364 (3)
C(8A)	2085 (2)	4129 (5)	3806 (3)
C(9A)	1818 (3)	6951 (6)	4223 (6)
O(2B)	5418 (2)	2879 (6)	6249 (2)
O(6B)	3885 (2)	1541 (5)	3590 (2)
N(1B)	4656 (2)	2112 (6)	4932 (2)
N(3B)	4483 (2)	1747 (5)	6254 (2)
N(7B)	2977 (2)	806 (4)	4543 (2)
N(9B)	3353 (2)	928 (4)	6001 (2)
C(1B)	5108 (3)	2568 (9)	4508 (3)
C(2B)	4885 (2)	2301 (7)	5838 (3)
C(3B)	4733 (3)	1848 (8)	7211 (3)
C(4B)	3857 (2)	1306 (6)	5749 (3)
C(5B)	3632 (2)	1217 (5)	4863 (3)
C(6B)	4033 (2)	1610 (6)	4379 (3)
C(8B)	2836 (2)	659 (6)	5254 (3)
C(9B)	3312 (3)	804 (8)	6874 (3)
N(41)	1371 (2)	911 (5)	5750 (3)
O(41)	987 (3)	2084 (6)	5479 (3)
O(42)	1702 (2)	867 (5)	6544 (3)
O(43)	1393 (3)	−230 (6)	5262 (4)
N(51)	3537 (2)	−4237 (5)	6100 (2)
O(51)	3512 (4)	−2815 (8)	5927 (5)
O(52)	3581 (6)	−5044 (9)	5588 (5)
O(53)	3621 (3)	−4797 (9)	6818 (3)
O(W)	6586 (2)	3961 (5)	6068 (2)

[a] Estimated standard deviations in the least significant figure are enclosed in parentheses in this and all following tables. [b] Parameters $\times 10^5$; for all other atoms, parameters $\times 10^4$.

B. $[(en)Pt(1,3,9\text{-}TMX)_2](PF_6)_2$. (a) Synthesis. For the preparation of the PF_6^- analogue, 105 mg of $[(en)Pt(1,3,9\text{-}TMX)_2](NO_3)_2 \cdot 2H_2O$ was dissolved in 25 mL of water and to this solution was added 45 mg of NH_4PF_6 in 10 mL of H_2O. Slow evaporation afforded sizable crystals of the PF_6^- salt. A density measurement ($CCl_4/CHBr_3$) and preliminary X-ray data were consistent with the formulation $[(en)Pt(1,3,9\text{-}TMX)_2](PF_6)_2$, which was later confirmed by the full X-ray analysis.

(b) Collection and Reduction of the X-ray Intensity Data. The crystal system (monoclinic) and the space group ($C2/c$) (systematic absences: hkl, $h + k = 2n + 1$; $h0l$, $l = 2n + 1$) were determined from preliminary oscillation and Weissenberg photography. The experimental techniques described above for the diffractometer data collection and reduction of the intensity data were also employed for this crystal. Crystal data and relevant data collection parameters are collected in Tables I and II.

(c) Solution and Refinement of the Structure. A structural solution for the 24 unique nonhydrogen atoms (the complex cation is required to possess $2(C_2)$ molecular symmetry) was readily formulated from standard Patterson–Fourier techniques. Several cycles of isotropic refinement led to an R value of 0.087. Two further cycles, employing anisotropic thermal parameters, reduced the R value to 0.055. A difference-Fourier map at this stage allowed the positioning of the 13 hydrogen atoms per asymmetric unit. Two subsequent cycles of refinement, holding the hydrogen atom parameters fixed, led to convergence (maximum shift/error of 0.8) and to a final R value of 0.044. The final weighted R and goodness-of-fit (with NO = 4275 nonzero observations and NV = 213 variables) values were 0.050 and 2.93, respectively. A final difference-Fourier synthesis contained residuals of up to 1.8 e/Å^3 in the vicinity of the F atoms of the PF_6^- anion, indicating librational disorder unaccounted for in the anisotropic thermal parameters for this group.

Table IV. Final Nonhydrogen Atom Coordinates for $[(en)Pt(1,3,9\text{-}TMX)_2](PF_6)_2$

atom	x	y	z
Pt[a]	50000	53747 (3)	25000
N(10)	5257 (3)	7006 (5)	3101 (2)
C(10)	5348 (4)	8379 (6)	2759 (3)
O(2)	4585 (3)	2422 (5)	5434 (2)
O(6)	3890 (3)	5397 (4)	3823 (2)
N(1)	4225 (3)	3861 (5)	4621 (2)
N(3)	5443 (3)	2209 (5)	4597 (2)
N(7)	5342 (3)	3852 (5)	3126 (2)
N(9)	6142 (3)	2110 (5)	3572 (2)
C(1)	3448 (5)	4398 (7)	4952 (3)
C(2)	4739 (4)	2804 (6)	4920 (2)
C(3)	6058 (5)	1221 (9)	4929 (3)
C(4)	5559 (3)	2630 (5)	3996 (2)
C(5)	5068 (3)	3698 (5)	3722 (2)
C(6)	4354 (3)	4411 (5)	4029 (2)
C(8)	5984 (3)	2898 (6)	3058 (2)
C(9)	6857 (4)	1015 (8)	3619 (3)
P	2991 (1)	656 (2)	3483 (0.8)
F(1)	3288 (3)	1179 (6)	4141 (2)
F(2)	2702 (5)	84 (8)	2827 (3)
F(3)	2036 (5)	503 (13)	3660 (4)
F(4)	3263 (9)	−875 (8)	3632 (4)
F(5)	3886 (5)	1115 (11)	3197 (3)
F(6)	2757 (9)	2273 (11)	3320 (4)

[a] Parameters $\times 10^5$; for all other atoms, parameters $\times 10^4$.

A final nonhydrogen atom coordinates are given in Table IV. Tables of anisotropic thermal parameters, hydrogen atom parameters, and final observed and calculated structure factor amplitudes are available.[19] The crystallographic computations for both analyses were performed with a standard set of computer programs.[20]

C. ^1H NMR Data. ^1H NMR spectra were recorded on a Varian CFT-20 spectrometer operating in the proton mode using standard Fourier-transform techniques. The solvent was D_2O, and the concentrations of the samples were ~0.10 M for the nitrate salt and ~0.05 M for the hexafluorophosphate salt. Employing a spectral width of 1202 Hz and a pulse width of 18 μs resulted in acquisition times of 1.7 s to accumulate 4K data points. The number of transients were 150 for the NO_3^- salt and 750 for the PF_6^- salt.

Results and Discussion

Molecular Geometry of the *cis*-$[(en)Pt(1,3,9\text{-}TMX)_2]^{2+}$ Cation in the Nitrate and Hexafluorophosphate Salts. In both compounds the $[(en)Pt(1,3,9\text{-}TMX)_2]^{2+}$ cation exhibits square-planar coordination geometry with the equatorial sites occupied by the nitrogen atoms of the en chelate and by the N(7) atoms of the two cis-bound 1,3,9-TMX bases. For the NO_3^- salt, the two 1,3,9-TMX ligands (labeled A and B) are crystallographically independent while in the PF_6^- salt the cation is required to possess $2(C_2)$ molecular symmetry. The molecular conformation of the $[(en)Pt(1,3,9\text{-}TMX)_2]^{2+}$ cations in the NO_3^- and PF_6^- salts are illustrated in Figure 2. In each case, a view is presented perpendicular to the mean PtN_4 coordination plane and (for the NO_3^- salt) along the pseudo-2-fold molecular axis or (for the PF_6^- salt) along the true, crystallographically imposed, molecular 2-fold axis. Details of the molecular dimensions are given in Table V.

The Pt–N(7A) and Pt–N(7B) (NO_3^- salt) bond lengths of 2.010 (3) and 2.021 (4) Å and the Pt–N(7) (PF_6^- salt) bond length of 2.018 (4) Å are pleasantly self-consistent and similar to those reported for $[(dien)Pt(Guo)]^{2+}$ (where dien is the tridentate chelate diethylenetriamine), 2.035 (13) Å,[21]

(20) Crystallographic programs employed: Wehe, Busing, and Levy's ORABS; Zalkin's FORDAP; Busin, Martin, and Levy's ORFLS (modified); Pippy and Ahmed's MEAN PLANE; Johnson's ORTEP.
(21) Melanson, R.; Rochon, F. D. *Can. J. Chem.* **1979**, *57*, 57.

Table V. Molecular Geometry for *cis*-[(en)Pt(1,3,9-TMX)$_2$](NO$_3$)$_2$·2H$_2$O and *cis*-[(en)Pt(1,3,9-TMX)$_2$](PF$_6$)$_2$[a]

(a) Primary Coordination Sphere about the Pt Atom for the NO_3^- Salt

Bond Lengths

Pt-N(10)	2.012 (4)	Pt-N(7A)	2.010 (3)
Pt-N(11)	2.026 (3)	Pt-N(7B)	2.021 (4)

Bond Angles

N(10)-Pt-N(11)	83.8 (2)	N(11)-Pt-N(7A)	174.2 (2)
N(10)-Pt-N(7A)	91.7 (1)	N(11)-Pt-N(7B)	95.5 (2)
N(10)-Pt-N(7B)	178.4 (2)	N(7A)-Pt-N(7B)	89.1 (1)

(b) Primary Coordination Sphere about the Pt Atom for the PF_6^- Salt

Bond Lengths

Pt-N(10)	2.029 (5)	Pt-N(7)	2.018 (4)

Bond Angles

N(10)-Pt-N(10′)	84.1 (2)	N(10)-Pt-N(7′)	175.2 (2)
N(10)-Pt-N(7)	92.2 (2)	N(7)-Pt-N(7′)	91.6 (2)

(c) en Chelate for the NO_3^- Salt

Bond Lengths

N(10)-C(10)	1.495 (7)	N(11)-C(11)	1.488 (7)
C(10)-C(11)	1.496 (8)		

Bond Angles

Pt-N(10)-C(10)	110.0 (3)	N(10)-C(10)-C(11)	108.3 (4)
C(10)-C(11)-N(11)	107.2 (4)	C(11)-N(11)-Pt	109.1 (3)

(d) en Chelate for the PF_6^- Salt

Bond Lengths

N(10)-C(10)	1.480 (8)	C(10)-C(10′)	1.514 (8)

Bond Angles

Pt-N(10)-C(10)	109.1 (4)	N(10)-C(10)-C(10′)	107.9 (4)

(e) 1,3,9-Trimethylxanthine Ligands

Bond Lengths

	NO_3^-				NO_3^-		
	A	B	PF_6^-		A	B	PF_6^-
N(1)-C(2)	1.396 (6)	1.394 (7)	1.395 (7)	N(9)-C(4)	1.372 (6)	1.366 (6)	1.368 (6)
N(1)-C(6)	1.389 (6)	1.401 (6)	1.404 (7)	N(9)-C(8)	1.369 (6)	1.351 (6)	1.353 (6)
N(1)-C(1)	1.474 (7)	1.467 (7)	1.461 (8)	N(9)-C(9)	1.465 (7)	1.477 (7)	1.469 (8)
N(3)-C(2)	1.396 (6)	1.384 (6)	1.387 (7)	O(2)-C(2)	1.218 (6)	1.214 (6)	1.201 (7)
N(3)-C(4)	1.354 (6)	1.373 (6)	1.382 (6)	O(6)-C(6)	1.227 (5)	1.216 (6)	1.223 (7)
N(3)-C(3)	1.463 (7)	1.465 (7)	1.472 (9)	C(4)-C(5)	1.365 (6)	1.356 (6)	1.359 (6)
N(7)-C(5)	1.389 (5)	1.390 (6)	1.377 (6)	C(5)-C(6)	1.427 (6)	1.433 (6)	1.430 (7)
N(7)-C(8)	1.320 (6)	1.325 (6)	1.310 (6)				

Bond Angles

	NO_3^-				NO_3^-		
	A	B	PF_6^-		A	B	PF_6^-
Pt-N(7)-C(8)	122.5 (3)	125.6 (3)	124.5 (3)	N(3)-C(2)-O(2)	121.7 (4)	121.3 (5)	121.2 (5)
Pt-N(7)-C(5)	131.7 (3)	129.7 (3)	129.4 (3)	N(1)-C(2)-N(3)	116.5 (4)	116.8 (4)	116.9 (5)
C(5)-N(7)-C(8)	105.8 (4)	104.2 (4)	105.5 (4)	N(3)-C(4)-C(5)	123.2 (4)	123.2 (4)	123.1 (4)
C(1)-N(1)-C(6)	117.7 (4)	116.6 (4)	117.1 (4)	N(3)-C(4)-N(9)	129.5 (4)	129.3 (4)	129.5 (4)
C(1)-N(1)-C(2)	114.7 (4)	116.2 (4)	116.0 (5)	N(9)-C(4)-C(5)	107.3 (4)	107.5 (4)	107.4 (4)
C(2)-N(1)-C(6)	127.2 (4)	127.2 (4)	126.8 (4)	C(6)-C(5)-N(7)	129.0 (4)	128.4 (4)	129.2 (4)
C(2)-N(3)-C(3)	117.0 (4)	117.3 (4)	117.7 (5)	C(6)-C(5)-C(4)	122.0 (4)	122.1 (4)	121.8 (4)
C(4)-N(3)-C(3)	124.3 (4)	123.8 (4)	123.5 (5)	N(7)-C(5)-C(4)	109.0 (4)	109.5 (4)	108.9 (4)
C(2)-N(3)-C(4)	118.7 (4)	118.5 (4)	118.7 (4)	C(5)-C(6)-O(6)	126.4 (4)	127.4 (4)	126.1 (5)
C(4)-N(9)-C(9)	131.6 (4)	131.7 (4)	131.4 (4)	N(1)-C(6)-O(6)	121.6 (4)	121.0 (4)	121.4 (5)
C(8)-N(9)-C(9)	122.2 (4)	122.4 (4)	122.8 (4)	C(5)-C(6)-N(1)	112.0 (4)	111.6 (4)	112.4 (4)
C(4)-N(9)-C(8)	106.2 (4)	105.9 (4)	105.6 (4)	N(7)-C(8)-N(9)	111.7 (4)	112.9 (4)	112.5 (4)
N(1)-C(2)-O(2)	121.7 (4)	121.9 (5)	121.9 (5)				

[a] Bond lengths in Å; bond angles in deg.

[(dien)Pt(Ino)]$^{2+}$, 2.029 (9) Å,[22] and *cis*-[(tn)Pt(Me-5′-GMP)$_2$], 2.021 (7) Å.[23] The remaining bond lengths and angles in the primary coordination spheres are also typical of those found in other Pt(II) complexes.[2]

The Pt---O(6) distances in both the NO_3^- salt [Pt---O(6A) = 3.413 (6) Å; Pt---O(6B) = 3.366 (6) Å] and the PF_6^- salt [Pt---O(6) = 3.354 (6) Å] are similar to those reported in related complexes with 6-oxopurine ligands[2,10] and do not suggest a significant participation of the 6-oxo group in the metal binding. In both compounds, however, the cation is somewhat stabilized by interligand hydrogen bonding utilizing the amino groups of the en chelate as donors and O(6) of the N(7)-bound 1,3,9-TMX ligands as acceptors. This type of interligand hydrogen bonding is commonly observed in such systems.[2,10] In the NO_3^- salt, these interligand hydrogen bonds are apparently slightly weaker [N(10)···O(6A) = 3.130 (8)

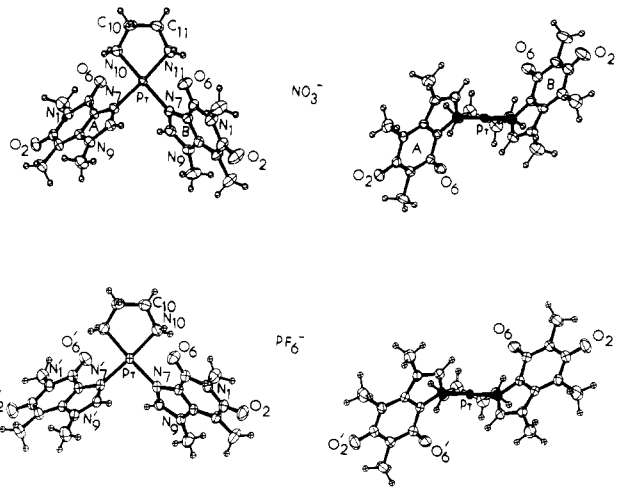

Figure 2. Views perpendicular to the mean PtN_4 coordination plane (left) and along the molecular 2-fold axis (right) of the *cis*-[(en)-Pt(1,3,9-TMX)$_2$]$^{2+}$ cations in the NO_3^- and the PF_6^- salts.

(22) Melanson, R.; Rochon, F. D. *Acta Crystallogr., Sect. B* **1978**, *B34*, 3594.
(23) Marzilli, L. G.; Chalilpoyil, P.; Chiang, C. C.; Kistenmacher, T. J. *J. Am. Chem. Soc.* **1980**, *102*, 2480 and references therein.

Table VI. Least-Squares Planes and the Deviations (in Å) of Individual Atoms from These Planes for $[(en)Pt(1,3,9\text{-}TMX)_2](NO_3)_2 \cdot 2H_2O$[a]

(a) Primary Coordination Sphere
$0.6710X + 0.6910Y - 0.2690Z = 1.1783$ Å

Pt	−0.015	N(10)	−0.038
N(7A)	0.047	N(11)	0.042
N(7B)	−0.038		

(b) 1,3,9-Trimethylxanthine Ligand A
$0.0054X - 0.2852Y + 0.9585Z = 4.7327$ Å

N(1A)	0.005	C(8A)	0.016
N(3A)	−0.034	Pt	0.042*
N(7A)	0.025	O(2A)	0.118*
N(9A)	−0.001	O(6A)	−0.116*
C(2A)	0.054	C(1A)	0.157*
C(4A)	−0.019	C(3A)	−0.124*
C(5A)	−0.015	C(9A)	−0.018*
(C6A)	−0.030		

(c) 1,3,9-Trimethylxanthine Ligand B
$-0.2776X + 0.9589Y - 0.0595Z = -0.8816$ Å

N(1B)	0.012	C(8B)	0.053
N(3B)	−0.054	Pt	0.265*
N(7B)	0.021	O(2B)	0.231*
N(9B)	−0.001	O(6B)	−0.054*
C(2B)	0.087	O(1B)	0.047*
C(4B)	−0.044	C(3B)	−0.055*
C(5B)	−0.044	C(9B)	−0.001*
C(6B)	−0.030		

[a] In each of the equations of the planes, X, Y, and Z are coordinates referred to the orthogonal axes a, b, and c^*. Atoms whose deviations are marked with an asterisk were given zero weight in calculating the planes; the atoms used to define the planes were given equal weight.

Å; N(11)···O(6B) = 3.045 (8) Å] than those in the PF_6^- salt [N(10)···O(6) = 2.993 (8) Å]. The difference in the apparent strength of these interligand hydrogen bonds is probably attributable to the different competitive intramolecular and intermolecular forces operative in the structures of the two salts.

Another consequence of the presence in the two structures of different counterions is the significant widening of the interbase dihedral angle from 70.6° for the NO_3^- salt to 87.3° for the PF_6^- salt. We shall return to this point and other conformational comparisons of the cations with other Pt(II)–6-oxopurine systems in detail later. We do note, however, that there is no intramolecular base/base interaction in either complex cation in spite of the fact that the high degree of methyl and oxo substitution on the 1,3,9-TMX ligand is known to enhance base/base interactions for the free ligand in solution.[24]

Molecular Dimensions of the 1,3,9-Trimethylxanthine Ligands. The bond lengths and angles in the N(7)-coordinated 1,3,9-TMX bases are presented and compared in Table V. There are no significant differences in the bond lengths for the three independent ligands and only one significantly different bond angle, namely, the Pt–N(7)–C(8) bond angle, which is smaller for the A ligand than the B ligand in the NO_3^- salt and is also smaller than the corresponding angle in the PF_6^- salt. Again this bond angle variation is probably a result of the differing environments about the 1,3,9-TMX bases in the two structures.

As with most purine bases, the nine-atom framework for the three independent 1,3,9-TMX ligands of the NO_3^- and the PF_6^- salts are measurably nonplanar (Tables VI and VII). The dihedral angles between the highly planar imidazole rings and the pyrimidine rings, which retain some degree of nonplanarity, are 2.3 and 4.9° for the ligands A and B of the NO_3^- complex and 4.1° for the PF_6^- complex. In both structures, the Pt atom shows marked deviations from the full purine planes. Whereas for the NO_3^- salt the Pt atom is displaced by 0.042 Å (ligand A) and 0.265 Å (ligand B), for the PF_6^- salt the displacement of the Pt atom is −0.220 Å. The sense of the above displacements is determined according to our previous convention[7] (a positive displacement means that the Pt atom is displaced from the plane of ligand A toward ligand B). The deviation of the other exocyclic substituents (the oxo and methyl groups) are also given in Tables VI and VII.

Table VII. Least-Squares Planes and the Deviations (in Å) of Individual Atoms from These Planes for $[(en)Pt(1,3,9\text{-}TMX)_2](PF_6)_2$[a]

(a) Primary Coordination Sphere
$0.9541X - 0.0000Y - 0.2996Z = 5.3589$ Å

Pt	0.000	N(10)	−0.053
N(7)	0.050	N(10)′	0.053
N(7)′	−0.050		

(b) 1,3,9-Trimethylxanthine Ligand
$-0.6472X - 0.6900Y - 0.3243Z = -9.7154$ Å

N(1)	0.052	C(8)	0.032
N(3)	−0.052	Pt	−0.220*
N(7)	−0.004	O(2)	0.071*
N(9)	0.034	O(6)	−0.063*
C(2)	0.028	C(1)	0.234*
C(4)	−0.024	C(3)	−0.239*
C(5)	−0.046	C(9)	0.011*
C(6)	−0.021		

[a] In each of the equations of the planes, X, Y, and Z are coordinates referred to the orthogonal axes a, b, and c^*. Atoms whose deviations are marked with an asterisk were given zero weight in calculating the planes; the atoms used to define the planes were given equal weight.

Table VIII. Distances (Å) and Angles (Deg) in the Interactions of the Type D-H···A[a]

D	H	D-H	A	H···A	D···A	∠D-H···A
(a) $[(en)Pt(1,3,9\text{-}TMX)_2](NO_3)_2 \cdot 2H_2O$						
N(10)	H(2N10)	0.88	O(2A)[a]	2.20	2.926 (8)	139
N(10)	H(2N10)	0.88	O(6A)	2.44	3.130 (8)	136*
N(10)	H(1N10)	0.88	O(41)[b]	2.38	3.092 (8)	139
N(10)	H(1N10)	0.88	O(42)[b]	2.10	2.944 (8)	161
N(11)	H(2N11)	0.90	O(6B)	2.39	3.045 (8)	129*
N(11)	H(2N11)	0.90	O(53)[c]	2.24	3.038 (8)	148
N(11)	H(1N11)	0.84	O(W)[d]	2.08	2.897 (8)	163
O(W)	H(1W)	0.89	O(2B)[e]	1.97	2.853 (8)	170
O(w)	H(2W)	0.97	O(52)[e]	1.87	2.747 (8)	150
(b) $[(en)Pt(1,3,9\text{-}TMX)_2](PF_6)_2$						
N(10)	H(2N10)	0.89	O(6)	2.16	2.993 (8)	157*

[a] Symmetry transforms (space group $P2_1/c$): (a) $-x, -1/2 + y, 1/2 - z$; (b) $x, 1/2 - y, -1/2 + z$; (c) $x, -1/2 - y, -1/2 + z$; (d) $1 - x, -y, 1 - z$; (e) x, y, z. An asterisk indicates intracomplex hydrogen bonds.

The Hexafluorophosphate and Nitrate Anions. Both the PF_6^- and the two independent NO_3^- anions show evidence of librational disorder, the respective fluorine and oxygen atoms of these groups showing varying degrees of exaggerated thermal motion. The average P–F bond distance is 1.54 (4) Å, with individual contributors ranging from 1.49 to 1.58 Å. The average cis F–P–F angle is 90 (5)° (range 81–96°). The average N–O bond length for the two NO_3^- anions is 1.19 (6) Å (range 1.09–1.24 Å), and the average O–N–O angle is 120 (4)° (range 113–125°).

Crystal Packing. The crystal structures for *cis*-$[(en)Pt(1,3,9\text{-}TMX)_2](NO_3)_2 \cdot 2H_2O$ and *cis*-$[(en)Pt(1,3,9\text{-}TMX)_2](PF_6)_2$ are shown in Figures 3 and 4, respectively. Intra- and intermolecular hydrogen-bonding interactions for

(24) Helmkamp, G. K.; Kondon, N. S. *Biochim. Biophys. Acta* **1968**, *157*, 242.

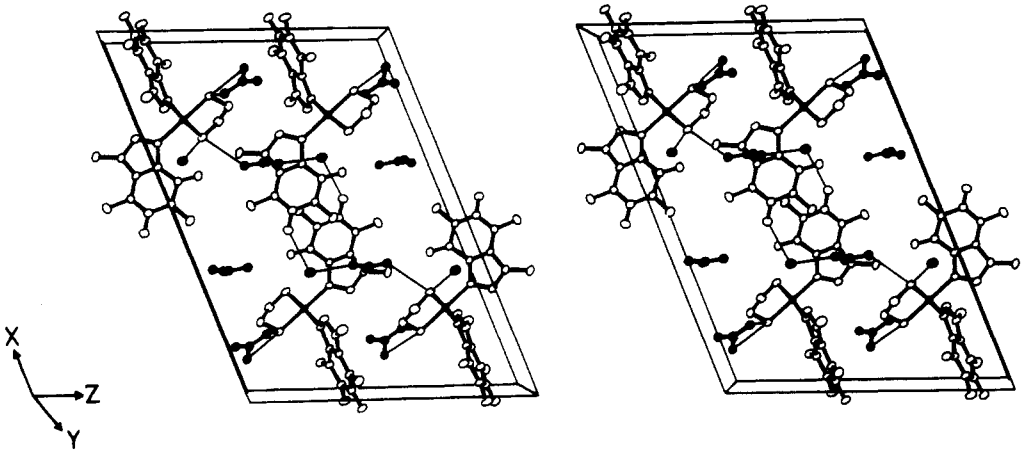

Figure 3. Stereoview of the crystal packing in the structure of *cis*-[(en)Pt(1,3,9-TMX)$_2$]$(NO_3)_2 \cdot 2H_2O$. Thin lines denote intermolecular hydrogen bonds. The thermal parameters of the oxygen atoms of the nitrate anions have been reduced for clarity.

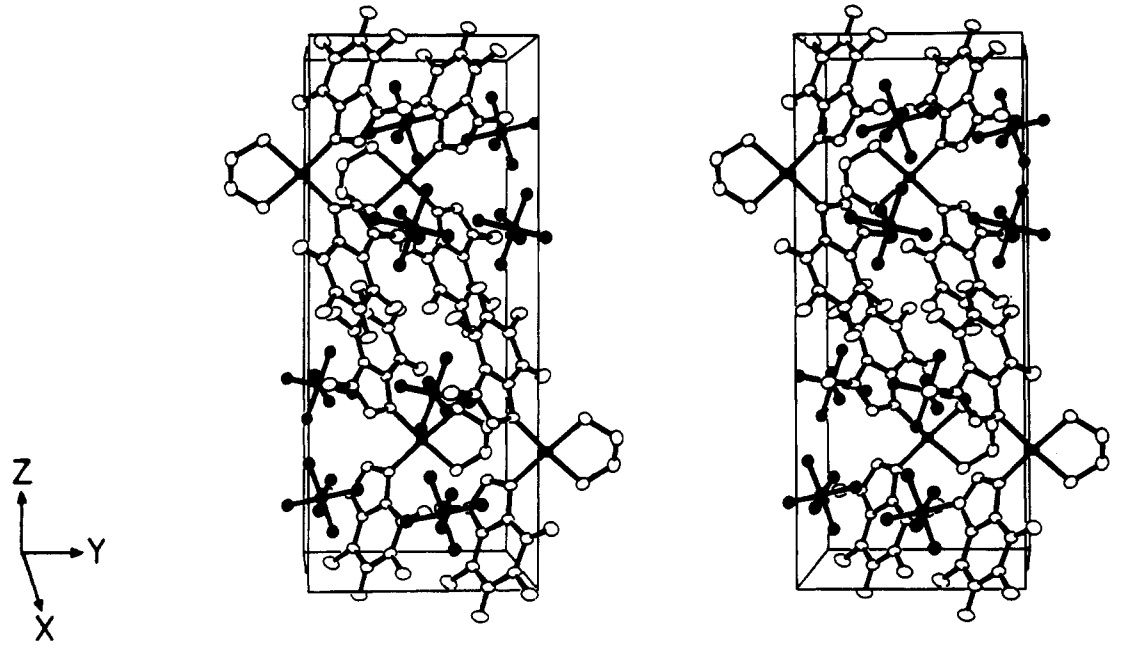

Figure 4. Stereoview of the crystal packing in the structure of *cis*-[(en)Pt(1,3,9-TMX)$_2$]$(PF_6)_2$. The thermal parameters of the fluorine atoms of the hexafluorophosphate anions have been reduced for clarity.

both structures are collected in Table VIII.

(a) *cis*-[(en)Pt(1,3,9-TMX)$_2$]$(NO_3)_2 \cdot 2H_2O$. The crystal structure for the NO_3^- salt is characterized by a network of hydrogen bonds involving the oxygen atoms of the nitrate anions, the located water molecule of crystallization, and the exocyclic oxygen atoms O(2) and O(6) of the purine bases A and B as acceptors and the amino groups of the en chelate as donors. Additional crystal stability is gained by electrostatic interactions between the nitrate groups and the complex cations. In particular, there are several close contacts between the oxygen atoms of the nitrate anions and the purine bases of the complex cation; see Figure 5. The planes of the nitrate anions are approximately perpendicular to those of the purine ligands (nitrate-41/base A dihedral angle = 71.6°; nitrate-51/base B dihedral angle = 79.2°). This is in contrast to the nearly parallel orientation of the nitrate groups to the pyrimidine ring planes in the structure of *cis*-[$(NH_3)_2$Pt(1-methylcytosine)$_2$]$(NO_3)_2 \cdot$1-methylcytosine.[7] Thus, the nitrate anions appear to arrive at electrostatically favorable orientations in either a perpendicular or a parallel mode, with some $\pi-\pi$ interaction allowable in the latter.

(b) *cis*-[(en)Pt(1,3,9-TMX)$_2$]$(PF_6)_2$. For the structure of the PF_6^- salt, there are no apparent intermolecular hydrogen bonds and the extended crystal structure is primarily stabilized by electrostatic interactions. The packing of the PF_6^- anions with the purine bases is emphasized and compared to that shown by the nitrate anions in Figure 5.

In addition to there being no intramolecular base/base interactions in either compound as noted above, there is an absence of intermolecular base/base interaction—again in spite of the preponderance of methyl and oxo substituents on the purine bases. What is observed is a dominance of electrostatic interactions on both sides of the purine ligands to the preclusion of intramolecular or intermolecular base/base coupling.

^{1}H NMR Spectra. We have obtained the ^{1}H NMR spectra of crystals of the NO_3^- and the PF_6^- salts of the *cis*-[(en)Pt(1,3,9-TMX)$_2$]$^{2+}$ cation dissolved in D_2O. Chemical shift data for the platinated ligand as well as for the protonated and neutral 1,3,9-TMX bases are presented in Table IX. Assignment of the resonances for free and protonated 1,3,9-TMX has been given by Lichtenberg, Bergmann, and Neiman.[25] Since the methyl protons are not directly attached to the purine framework, only small shifts are observed for these resonances

(25) Lichtenberg, D.; Bergmann, F.; Neiman, Z. *J. Chem. Soc. C* **1971**, 1676.

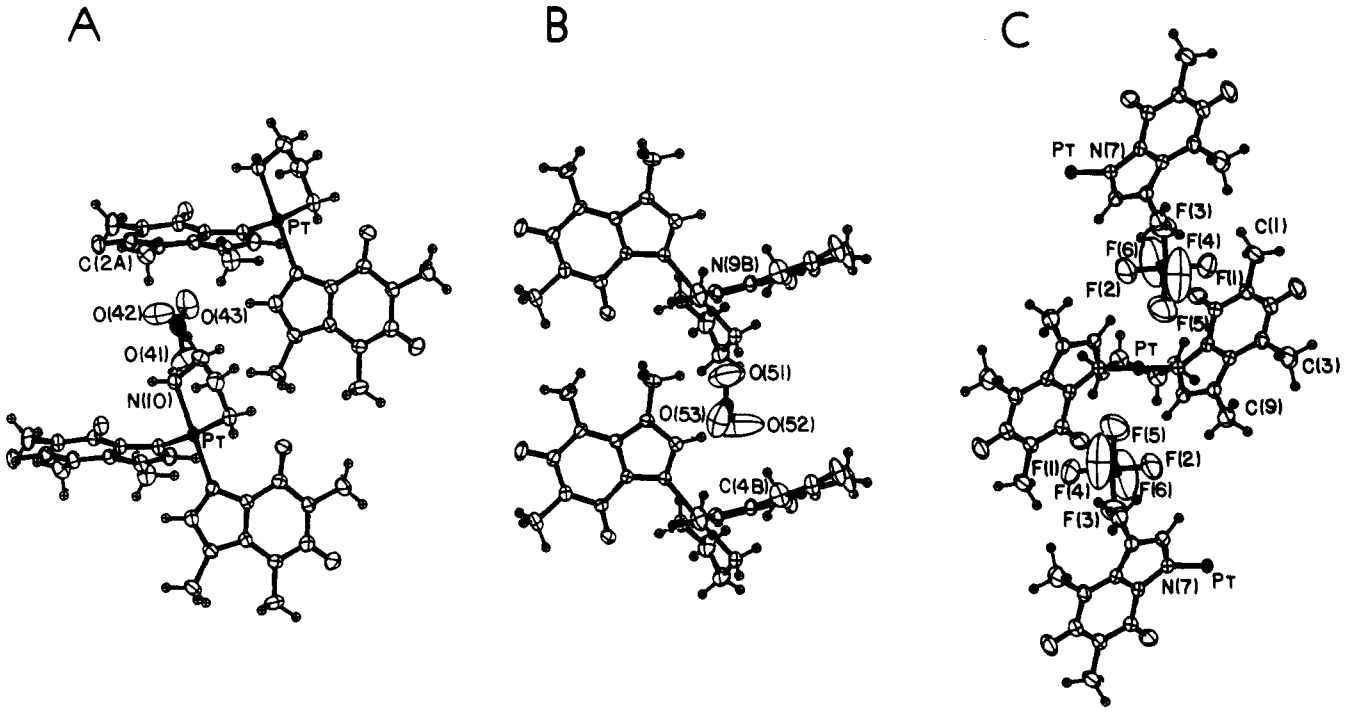

Figure 5. Anion/cation intermolecular interactions in the NO_3^- (parts A and B) and the PF_6^- (part C) salts.

Table IX. Proton Chemical Shift Data (D_2O; δ, Downfield from *tert*-Butyl Alcohol) for *cis*-$[(en)Pt(1,3,9\text{-}TMX)_2]^{2+}$

	H(8)	1-CH_3	3-CH_3	9-CH_3
1,3,9-TMX[a]	6.37	2.06	2.49	2.72
$[(en)Pt(1,3,9\text{-}TMX)_2]^{2+}$, NO_3^- salt[c]	6.76[b]	2.15	2.50	2.76
$[(en)Pt(1,3,9\text{-}TMX)_2]^{2+}$, PF_6^- salt[d]	6.76[b]	2.15	2.49	2.75
1,3,9-TMXH$^+$ [e]	7.47	2.13	2.57	2.95

[a] Assignments taken from ref 25. [b] $J_{^{195}Pt-^1H} = \sim 23$ Hz; we also note that δ = 1.57 and $J_{^{195}Pt-^1H} = 45$ Hz for the methylene protons of the en ligand. [c] Approximately 0.10 M. [d] Saturated solution, ~0.05 M. [e] Approximately a 2-fold excess of trifluoroacetic acid.

upon protonation or platination, and this allows the resonances for the cationic species to be assigned with reasonable confidence.

As expected, the H(8) proton shows the largest shift on either platination (0.39 ppm downfield) or protonation (1.10 ppm downfield), because H(8) is close to the protonated or platinated N(7) ring site. Coupling between ^{195}Pt and H(8) is also observed, and the coupling constant (~23 Hz) is consistent with measurements on other N(7)-bound purine systems.[26]

An interesting aspect of these spectra is that the change in chemical shifts for the methyl protons between the free base and the protonated base is different from that between the free base and the platinated base. The order for the protonated species 9-CH_3 > 3-CH_3 ≈ 1-CH_3 is naively expected (and observed earlier by Lichtenberg et al.[25]) since the 9-CH_3 group is bonded to the imidazole ring and protonation occurs at the N(7) position. In contrast, the order for the platinated species is 1-CH_3 > 9-CH_3 > 3-CH_3.[27] The unexpected order for the platinated species is further compounded by the fact that Chu and Tobias[28] observed only a small *upfield* shift (~0.05 ppm) for the 1-CH_3 protons of 1-methylinosine upon coordination to $[(ND_3)_2Pt(H_2O)_2]^{2+}$.

Conformational Features of *cis*-Bis(N(7)-bound 6-oxopurine)platinum(II) Complexes. As noted in the Introduction, there are three main types of cross-linking modes by which cis Pt(II) complexes may interact with G–C-rich regions of polynucleotides. In the previous sections, we have described in detail the molecular and crystal structures of the coordination compounds *cis*-$[(en)Pt(1,3,9\text{-}TMX)_2](NO_3)_2 \cdot 2H_2O$ and *cis*-$[(en)Pt(1,3,9\text{-}TMX)_2](PF_6)_2$, which are models for the type 1 interaction. A number of other model systems for this mode have been studied X-ray crystallography over the past few years. These models include the Cl^-/ClO_4^- and Cl^-/I^- salts[29] of $[(en)Pt(Guo)_2]^{2+}$, the sodium salt[30] of *cis*-$[(NH_3)_2Pt(5'\text{-}IMP)_2]^{2-}$, and the neutral species $[(tn)Pt(Me\text{-}5'\text{-}GMP)_2]$.[23]

Adopting our previously described convention,[7] we compare for all of the above systems the interbase dihedral angle (B/B′) and the base/PtN_4 dihedral angles (B,B′/PtN_4) and the perpendicular displacement of the Pt atom from the plane of the bases to which it is bonded. A compendium of these conformational parameters is given in Table X, and the dihedral angles are illustrated in Figure 6. We note that as the interbase dihedral angle B/B′ increases so do the B,B′/PtN_4 coordination-plane dihedral angles. This trend is opposite to that displayed for *cis*-bis(ring-bound pyrimidine)platinum(II) complexes. We have rationalized the latter trend on the basis of intracomplex steric factors, which are determined by the number of exocyclic substituents ortho to the Pt binding sites.[7] A rationalization of the trend exhibited by the *cis*-bis(N-(7)-bound 6-oxopurine)platinum derivatives (which in a formal sense have no substituents other than H ortho to the Pt binding site) clearly requires a different approach. For these com-

(26) (a) Kong, P. C.; Rochon, F. D. *J. Chem. Soc., Chem. Commun.* **1975**, 599. (b) Kong, P. C.; Theophanides, T. *Inorg. Chem.* **1974**, *13*, 1167. (c) Hadjiliadis, N.; Theophanides, T. *Inorg. Chim. Acta* **1976**, *16*, 77.

(27) Because of the relatively small chemical shift differences between resonances for the free and platinated 1,3,9-TMX base, we titrated the free base with $[(en)Pt(H_2O)_2]^{2+}$ in D_2O. At low Pt/base concentrations and at short reaction times, we observed resonances for both the free base and the platinated base and derive exactly the same chemical shift differences obtainable from Table IX.

(28) Chu, G. Y. H.; Tobias, R. S. *J. Am. Chem. Soc.* **1976**, *98*, 2641.

(29) (a) Cramer, R. E.; Dahlstrom, P. L.; Seu, J. T.; Norton, T.; Kashiwagi, M. *Inorg. Chem.* **1980**, *19*, 148. (b) Gellert, R. W.; Bau, R. *J. Am. Chem. Soc.* **1975**, *97*, 7379.

(30) Kistenmacher, T. J.; Chiang, C. C.; Chalilpoyil, P.; Marzilli, L. G. *J. Am. Chem. Soc.* **1979**, *101*, 1143.

Table X. Relevant Conformational Parameters for *cis*-Bis(N(7)-bound purine ring)platinum(II) Complexes

complex	ref	dihedral angles, deg B/B′	B/PtN$_4$	B′/PtN$_4$	Δ Pt,[c] Å	Δ Pt′,[c] Å
[(en)Pt(1,3,9-TMX)$_2$]$^{2+}$, PF_6^- salt[a]	this study	87.3	121.4		−0.220	
[(en)Pt(1,3,9-TMX)$_2$]$^{2+}$, NO_3^- salt	this study	70.6	116.8 (TMX_A)	119.5 (TMX_B)	+0.042 (TMX_A)	+0.265 (TMX_B)
[$(NH_3)_2$Pt(Guo)$_2$]$^{2+}$, Cl^-/ClO_4^- salt	29a	73.7	70.2 (Guo_A)	73.9 (Guo_B)	+0.090 (Guo_A)	+0.238 (Guo_B)
[(en)Pt(Guo)$_2$]$^{2+}$, Cl^-/I^- salt[a]	29b	70.8	73.1		+0.198	
[(tn)Pt(Me-5′-GMP)$_2$]^0 [a]	23	39.6	53.0		+0.541	
$(NH_3)_2$Pt(5′-IMP)$_2$]$^{2-}$, Na salt[a]	30[b]	40.7	61.8		+0.659	

[a] Molecular 2-fold symmetry present. [b] 86% Pt occupancy. [c] Displacement of the Pt atom from the nine-atom purine plane.

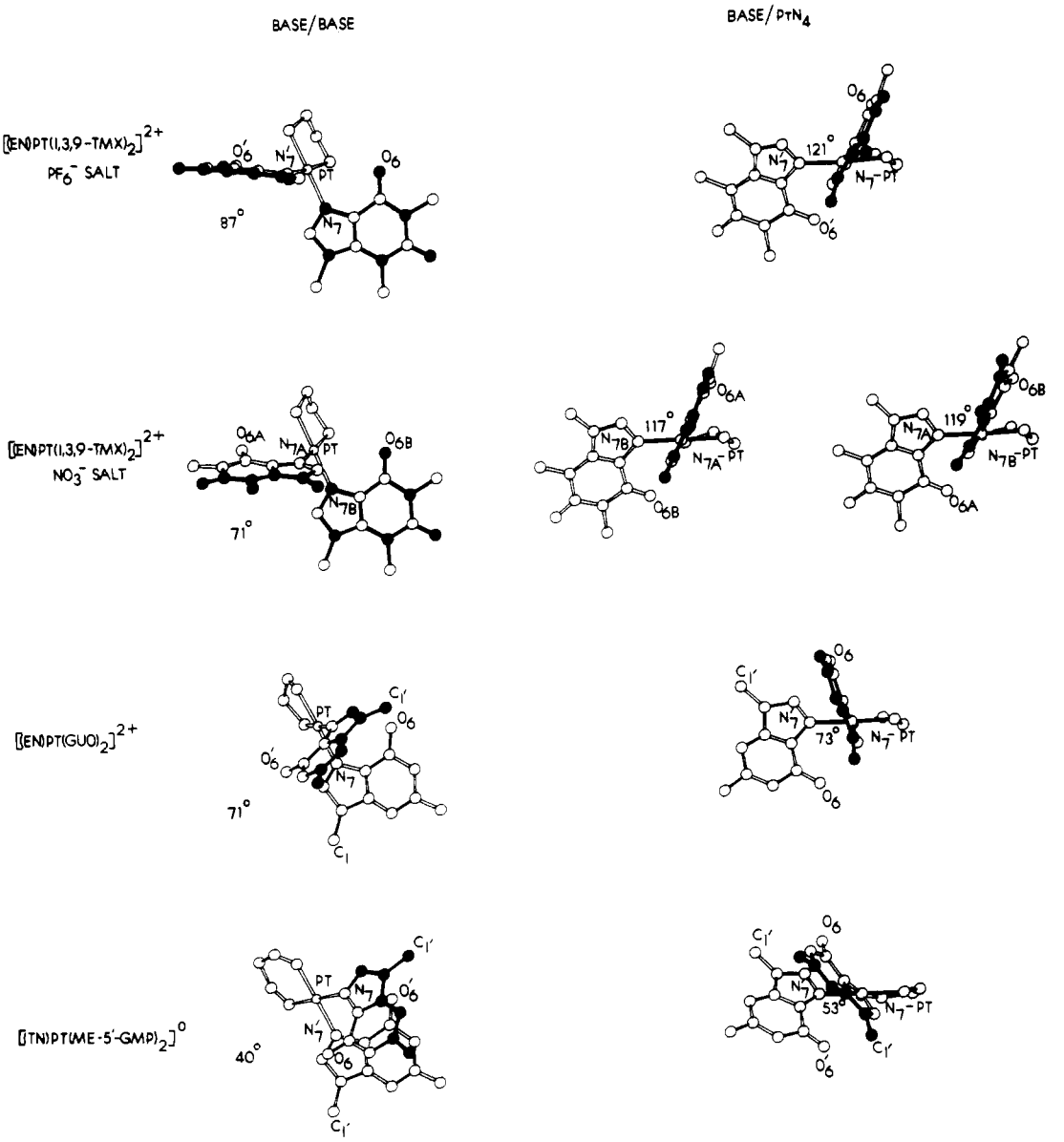

Figure 6. Illustrations and magnitudes for the base/base and base/PtN$_4$ intramolecular dihedral angles for four *cis*-bis(N(7)-bound 6-oxopurine)platinum(II) complexes. Ligand abbreviations employed are as follows: 1,3,9-TMX = 1,3,9-trimethylxanthine; GUO = guanosine; ME-5′-GMP = the phosphate methyl ester of guanosine 5′-monophosphate; en = ethylenediamine; tn = trimethylenediamine.

pounds it is readily apparent that both the B/B′ and the B,B′/PtN$_4$ dihedral angles tend to increase on going from systems involving nucleotide ligands through nucleoside ligands to those for nucleobase derivatives such as 1,3,9-TMX. For the nucleotide complexes, there is a clear preference for a highly significant intracomplex base/base interaction both in the presence (*cis*-[$(NH_3)_2$Pt(5′-IMP)$_2$]$^{2-}$) and in the absence ([(tn)Pt(Me-5′-GMP)$_2$]^0) of counterions. This attractive intracomplex base/base interaction is reflected in the relatively small B/B′ and B,B′/PtN$_4$ angles—the interaction being facilitated by rotation about the Pt–N(7) bond.

For the nucleoside complexes, the higher values for the conformational dihedral angles indicate less intracomplex base/base interaction. However, the relative orientation of the base ligands, Figure 6, suggests that, although weaker, such an interaction is still present. In these systems, the reduced intracomplex base/base interaction is probably due to competition with intermolecular base stacking.[23]

The simplest model for the type 1 cross-linking mode should be systems containing two nucleobase derivatives. In the PF_6^-

and NO_3^- salts studied here, the B/B′ and the B,B′/PtN_4 dihedral angles are relatively large and indicate no intracomplex base/base interaction. In addition, as noted above, there are no intercomplex base-stacking interactions. Instead we find considerable anion interaction with the coordinated bases; see Figure 3-5. For these 1,3,9-TMX complexes, the presence of different counterions in the crystal structure does have a significant influence on the magnitude of the B/B′ dihedral angle—the angle for the PF_6^- salt being nearly 17° larger than that for the NO_3^- salt.

Thus, we conclude for *cis*-bis(N(7)-bound 6-oxopurine)-platinum(II) model systems representing the type 1 cross-linking mode that the primary conformational features are determined by competition between intracomplex (base/base, hydrogen bonding) and intercomplex (base/base, base/counterion, hydrogen bonding) interactions. Intracomplex base/base interactions apparently become more important on going from nucleobase complexes to nucleoside complexes to nucleotide complexes. A factor that may be important with regard to the latter complexes is the common occurrence of an O(phosphate)···H–O–H···O(6) hydrogen-bonding scheme.[23] However, a complete understanding of the conformational aspects of type 1 model complexes is yet to be achieved. More work is clearly needed to fully rationalize all factors influencing the conformations of nucleotide, nucleoside, and nucleobase systems.

Acknowledgment. This investigation was supported by the National Institutes of Health, Public Health Service Grant GM 29222. We thank Matthey Bishop, Inc., for a loan of K_2PtCl_4.

Registry No. [(en)Pt(1,3,9-TMX)$_2$]$(NO_3)_2 \cdot H_2O$, 79855-87-1; [(en)Pt(1,3,9-TMX)$_2$]$(PF_6)_2$, 79872-71-2; (en)PtI_2, 23858-10-8.

Supplementary Material Available: Tables of nonhydrogen anisotropic thermal parameters, parameters for the hydrogen atoms, and calculated and observed structure factor amplitudes for each reported structure (78 pages). Ordering information is given on any current masthead page.

Notes

Contribution from the Chemistry Department, University of Tasmania, Hobart TAS 7001, Australia

A Simple Method of Estimating the Change in Metal–Ligand Bond Length Accompanying a Rearrangement of the d Electrons in a Transition-Metal Complex

M. A. Hitchman

Received April 24, 1981

It is well-known that a change in the occupancy of the antibonding d orbitals directed toward the ligands in a complex such as often occurs upon light absorption or a high/low-spin interconversion is generally accompanied by a significant alteration in the equilibrium metal–ligand bond distance.[1] A closely related problem concerns the Jahn–Teller distortions associated with an unequal occupancy of the e_g orbitals of an octahedral complex, which are conventionally treated quantitatively by expanding the potential energy of the molecule as a function of the Jahn–Teller active vibrational mode.[2] The purpose of the present note is to point out that an analogous procedure may be used to derive the difference in bond length between two forms of a metal complex having different d-electron configurations, in this case by expanding the potential energy difference between these as a function of the totally symmetric metal–ligand stretching mode.

If it is assumed that the energy separation Δ between the d orbitals involved in the electron change depends inversely on some power n of the bond distance, the change in bond length δr is related to the force constant f of the symmetric stretch by the equation[3]

$$\delta r \simeq \frac{nm\Delta}{fr_0N} \qquad (1)$$

which is derived in the Appendix. Here, m is the number of electrons involved in the change, r_0 is the initial bond distance, and N is the number of ligand atoms bonded to the metal. Simple bonding theories, both covalent and electrostatic, and experimental evidence suggest that $n \simeq 5$ at least for the d orbital splitting complex.[4] Using this value, it is of interest to see how the bond length changes estimated with use of eq 1 agree with those deduced for transitions between ground and excited d configurations from electronic spectroscopy and observed by X-ray crystallography for complexes having different spin ground states. It may be noted that a very similar expression to that given in eq 1 may be derived to describe the distorted geometries that result from coupling with Jahn–Teller active modes for metal ions with orbitally degenerated electronic states; this will be the subject of a future publication.

Bond Length Changes Accompanying "d–d" Excitations

It is well established that the width of a "d–d" absorption band depends upon the difference in the equilibrium bond length between the ground and excited state.[1] Recently, quantitative estimates of these differences have been deduced from the spectra of several complexes and the values obtained are shown in Table I together with those estimated with use of eq 1. In each compound the transition is between the $d_{x^2-y^2}$ and d_{xy} orbitals or their equivalents in energy. A single electron is involved in every case except that of $[Cs_2NiCl_4] \cdot CsCl$, for which, because of the effects of interelectron repulsion, $m = 1.75$,[5] and the $^5T_{2g} \leftarrow {}^1A_{1g}$ transition of $Co(NH_3)_6^{3+}$ for which $m = 2$. Agreement between the two sets of values is generally good, the only marked discrepancy occurring for the planar $CuCl_4^{2-}$ ion,[6] for which the value obtained with use of eq 1 is about twice that derived from the

(1) See, e.g., C. K. Jørgensen, "Absorption Spectra and Chemical Bonding in Complexes", Pergamon Press, 1962, p 98.
(2) D. Reinen and C. Friebel, *Struct. Bonding (Berlin)*, **37**, 1 (1979), and references therein.
(3) An essentially similar expression, applying just to an octahedral complex, is given in ref 7.
(4) D. W. Smith, *Struct. Bonding (Berlin)*, **35**, 105 (1978), and references therein.
(5) T. W. Couch and G. P. Smith, *J. Chem. Phys.*, **53**, 1336 (1970). The number of electrons involved in the relevant transition was obtained from the eigenvectors of the appropriate matrix, and the change in bond length was estimated from the reported relative intensities of the vibrational components of the band due to the $^3A_2 \leftarrow {}^3T_1(F)$ transition with use of the tables in: J. R. Henderson, R. A. Willett, M. Muramoto, and D. C. Richardson, "Douglas Reports SM-45807, Jan. 1964".
(6) M. A. Hitchman and P. Cassidy, *Inorg. Chem.*, **18**, 1745 (1979).

0020-1669/82/1321-0821$01.25/0